JOURNAL OF OPTOELECTRONICS AND ADVANCED MATERIALS, Vol. 11, No. 7, July 2009, p. 988 - 993

Surface roughness of low-temperature polycrystalline silicon prepared by excimer laser crystallization

CHIL-CHYUAN KUO
Department of Mechanical Engineering, Ming Chi University of Technology
No. 84, Gungjuan Road, Taishan Taipei Hsien 243, Taiwan

Surface roughness of polycrystalline silicon (poly-Si) films fabricated by both frontside excimer laser crystallization (ELC) and backside ELC are investigated by atomic force microscope. The results show that surface roughness of poly-Si films achieved by backside ELC is lower than that by frontside ELC in three distinct regrowth regimes. The root mean square surface roughness of poly-Si films for frontside ELC and backside ELC in the super lateral growth regime is 21.192 nm and 16.263 nm, respectively. Backside ELC seems to be a good candidate for batch production of low-temperature polycrystalline silicon thin-film transistors under the conditions including same maximum grain size of poly-Si films for both frontside ELC and backside ELC, higher laser efficiency, and lower surface roughness of poly-Si films.

(Received June 18, 2009; accepted July 20, 2009)

Keywords: Surface roughness, Low-temperature polycrystalline silicon.Excimer laser crystallization

1. Introduction

In recent years, the polycrystalline silicon (poly-Si) thin-film transistors (TFTs) have widely been employed in many applications, especially in active matrix liquid crystal displays (AMLCDs) [1]. The major advantage of applying poly-Si TFTs to AMLCDs is the increase in carrier mobility, as well as the ability to integrate the pixel switching elements and peripheral driving circuit on the same substrate [2]. The deposition of poly-Si films on glass at low temperatures can be performed by direct growth of the polycrystalline material on the substrate using chemical vapor deposition (CVD). The major drawback of this technique is that the grain size of poly-Si films is not sufficiently large to realize the high-performance low-temperature polycrystalline silicon thin-film transistors (LTPS TFTs). Historically, the solid-phase-crystallization (SPC) is the first technology for fabricating poly-Si films with large grain for display application, followed by the development of laser annealing crystallization [3]. As well known from the literature [4], SPC is a simple technique of heating the sample up to 500-600 °C, but the major drawback of this technique is that the long processing time needed for complete crystallization. Thus, excimer laser crystallization (ELC) has currently become a state-of-the-art technology for the fabrication of high-performance poly-Si TFTs on inexpensive glass substrate because this technology produces crystallization films of higher quality in a very fast process [5]. It is well known that the most common approach to crystallizing the amorphous silicon (a-Si) is conventional frontside ELC [6-9]. The working principle of frontside ELC means the a-Si films being irradiated directly by the excimer laser beam. Conversely, backside ELC denotes the a-Si films are irradiated by the transmitted excimer laser through substrate and SiO_2 films. Backside ELC can be employed in this study because the XeF excimer laser whose wavelength is close to near ultraviolet can pass through the glass substrate. Unfortunately, the formation of ridge [10] or pillar [11] in the GBs cannot be avoided after ELC. The surface roughness of poly-Si films caused by ridge formation has become an important issue because it degrades significantly the electrical characteristics of LTPS TFT_S [11]. Although the issues regarding the surface roughness of poly-Si films fabricated by ELC have been studied for many years [12-14], none of these investigations paid particular attention to the difference in surface roughness of poly-Si films between frontside ELC and backside ELC. In order to clarify the difference in surface roughness achieved by the two ELC approaches, poly-Si films crystallized under both conditions are investigated extensively using atomic force microscope (AFM), field-emission scanning electron microscopy (FE-SEM), and high-resolution transmission electron microscope (HR-TEM). An analysis of surface roughness of poly-Si films between frontside ELC and backside ELC is presented. The best approach for batch production of LTPS TFTs using ELC is suggested.

2. Experimental details

The substrate choice for experimental study is

inexpensive Corning Glass 1737. Hydrogenated a-Si thin films (a-Si: H) of 90-nm-thick are deposited on glass substrate covered with a 300-nm-thick SiO_2 layer by plasma-enhanced chemical vapor deposition (PECVD). The a-Si: H films are then dehydrogenated by thermal treatment at 500 °C for 2 hours for removing excess hydrogen in order to prevent the ablation caused by sudden hydrogen eruption during ELC. The samples are then held in self-closing tweezers at the end of a cantilever beam fixed on a motorized x-y linear translation stage (resolution = 0.625 μm). The movement of the focusing lens (focus = 100 mm) fixed on a motorized z-axis linear translation stage is precisely controlled to adjust the desired excimer laser energy density for ELC. To enhance the efficiency of ELC, the movement of the three-axis (X−Y−Z) motorized translation stages can be accurately manipulated using the man- machine interface. A Joule meter (Vector H410 SCIENTECH) is employed to calibrate the output energy of excimer laser pulse before ELC. Since the excimer laser beam (XeF,λ= 351 nm, LAMBDA PHYSIK COMPex 102) can pass through the glass substrate, the backside ELC can be performed in this study. No substrate heating is employed. a-Si thin films are crystallized by a single-shot XeF excimer laser with 25-ns pulse duration at room temperature in air. Figure 1 is a schematic illustration of both frontside ELC and backside ELC. The incident excimer laser beam is generally perpendicular to the surface of Si thin films. As can be seen, a-Si films are irradiated directly by excimer laser beam for frontside ELC. For backside ELC, the a-Si films are irradiated by the transmitted excimer laser through substrate and SiO_2 films. A stainless-steel slit mask of around 2 × 15 mm^2 is employed to transform the incident Gaussian beam into a rectangular beam spot with pulse-to-pulse energy variations within ± 10 %. The size of the beam spot can be controlled by changing the working distance between the focusing lens and the sample surface.

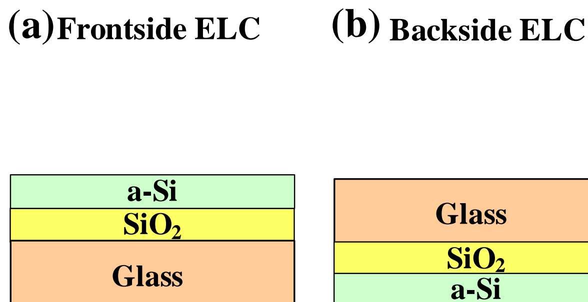

Fig. 1. Schematic illustration of (a) frontside ELC and (b) backside ELC.

After ELC, the microstructural analysis of annealed poly-Si films are performed by FE-SEM (Oxford JEOL JSM-6500F), AFM (Digital Instruments, Dimension 3100), and HR-TEM (JEOL JEM-2010). Before FE-SEM observation, the crystallized silicon films are Secco-etched (50 % HF: H_2O: CrO_3 = 200 cc: 100 cc: 1.5 g) in order to highlight the grain boundaries (GBs) and intra-grain defects [15]. The acceleration electron beam energy for SEM and TEM experiment are 15 kV (resolution 1.5 nm) and 200 kV (point resolution 0.23 nm), respectively. The corresponding surface roughness measurements of poly-Si films are performed by an AFM in the tapping mode (scan rate = 1 Hz). The rectangular Si tip operated with a resonant frequency of 322.656 kHz is used as a probe with a spring constant of 40 N/m. All micrographs have been scanned in constant force mode at ambient temperature and pressure. The root-mean-square (RMS) roughness of poly-Si films can be determined by the following equations:

$$\mathrm{RMS}=\sqrt{\frac{\sum_{i=1}^{n}(Z_i - Z_{ave})^2}{n}} \quad (1)$$

$$Z_{ave}=\frac{\sum_{i=1}^{n} Z_i}{n} \quad (2)$$

where Z_i is the height of the i_{th} micrograph points, Z_{ave} is the average height, and n is the total number of micrograph points used.

3. Results and discussion

Fig. 2 shows the SEM images of Secco-etched poly-Si films in four distinct regrowth regimes. A detailed description about the phenomena of four distinct regrowth regimes can be found in my previous investigations [16, 17]. As can be seen, the amorphous regions of the silicon thin films have been etched away, leaving only poly-Si on the glass substrate. In the partial melting regime, there is an increase in the grain size of poly-Si films with increasing excimer laser energy density. In particular, the grain size of poly-Si films reaches the maximum because of the super lateral growth (SLG) nucleation in the near-complete melting regime. The detailed recrystallization mechanism of this unique phenomenon has been described elsewhere [6-8]. When the laser energy density exceeds the ablation excimer laser energy density, some a-Si films will evaporate, resulting in poor morphology of the sample.

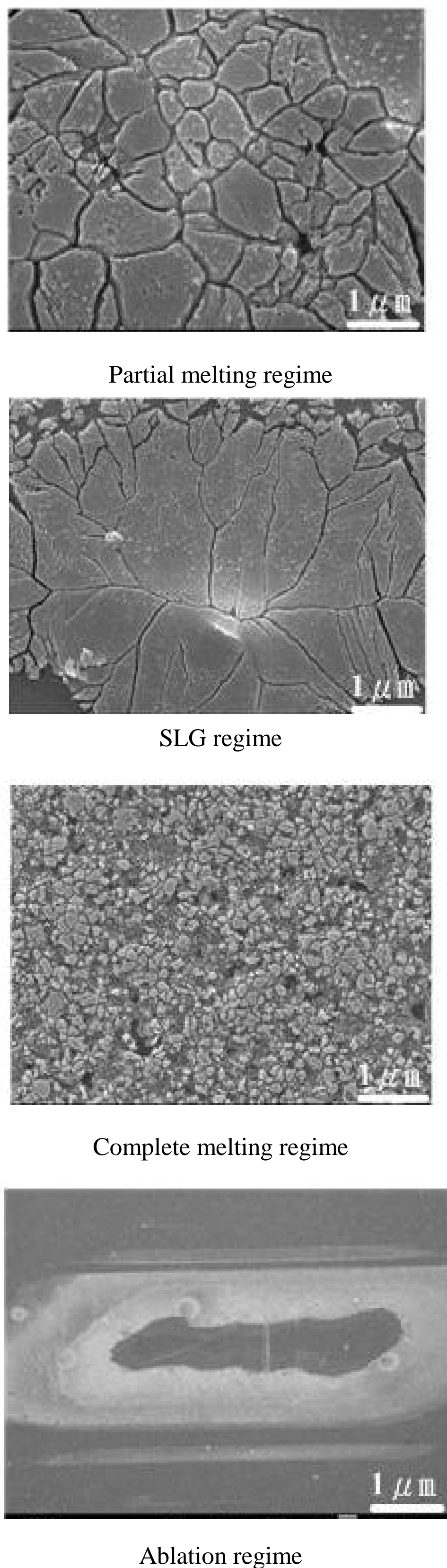

Fig. 2. FE-SEM images of Secco-etched poly-Si films in four distinct regrowth regimes. Excimer laser energy density for the parting melting regime, SLG regime, complete melting regime, and ablation regime is 130 mJ/cm^2, 190 mJ/cm^2, 210 mJ/cm^2, and 230 mJ/cm^2, respectively.

In order to clarify the difference in surface roughness between frontside ELC and backside ELC, the surface roughness of poly-Si films fabricated by both frontside ELC and backside ELC are extensively investigated by AFM. Owing to an excimer laser pulse inherent with Gaussian beam profile, the liquid Si has a steep lateral temperature gradient. Figure 3 shows the typical AFM micrographs of poly-Si films irradiated by the excimer laser energy density that causes the a-Si film complete melting for (a) frontside ELC and (b) backside ELC. As shown in Figure 4, the area (30 μm ×30 μm) used for estimating RMS roughness is in the vicinity of near-complete melting regime of the spot size. The rectangular shape indicates the spot size after excimer laser crystallization. Indeed, the spot size varies in different excimer laser energy density. The dimension of the spot size irradiated of excimer laser energy density of 210 mJ/cm^2 is around 2 mm × 1.5 mm. Two important characteristic phenomena can be inferred from Figure 3. First, the surface roughness of poly-Si films depend sensitively on the incident excimer laser energy density, revealing that different excimer laser energy densities result in different surface roughness of poly-Si films in the pattern after ELC. Second, the maximum surface roughness of poly-Si films is observed in the SLG regime (i.e. grain size of poly-Si is several times the Si film thickness), revealing that surface roughness of poly-Si films increases with the increase in grain size of poly-Si films. This is also confirmed by the corresponding FE-SEM analysis in another previous investigation [16]. Figure 5 shows the surface topography measured by AFM of poly-Si films in the SLG regime for both frontside ELC and backside ELC. The area used for estimating RMS roughness is in the center of the spot size. Excimer laser energy density for frontside ELC and backside ELC is 190 mJ/cm^2 and 175 mJ/cm^2, respectively. The RMS surface roughness of poly-Si for frontside ELC and backside ELC in the SLG regime is 21.192 nm and 16.263 nm, respectively. This result indicates that the RMS roughness in the SLG regime of the laser-irradiated region for backside ELC is lower than that for frontside ELC. The increase in surface roughness of poly-Si films is mainly caused by the ridge or pillar formed in the GBs after ELC. The ridge or pillar is formed by the impingement of grains grown laterally in the opposite direction. A possible mechanism for the formation of ridge or pillar in the GBs is proposed by Fork et al. [9] and Shih et al. [10], respectively.

To investigate quantitatively the changes in surface roughness of poly-Si films in three distinct regrowth regimes, some patterns are investigated in this work. The average surface roughness in three distinct regrowth regimes for both ELC is summarized in Figure 6. As can be seen, the average RMS roughness in the partial melting, SLG and complete melting regimes of frontside ELC is higher than that of backside ELC. This result reveals that surface roughness of poly-Si films achieved by backside ELC is lower than that by frontside ELC because the

massive mass transport effects is triggered during solidification process in frontside ELC [18]. This phenomenon is also confirmed by the corresponding cross-sectional TEM images in the SLG regime, as shown in Fig. 7.

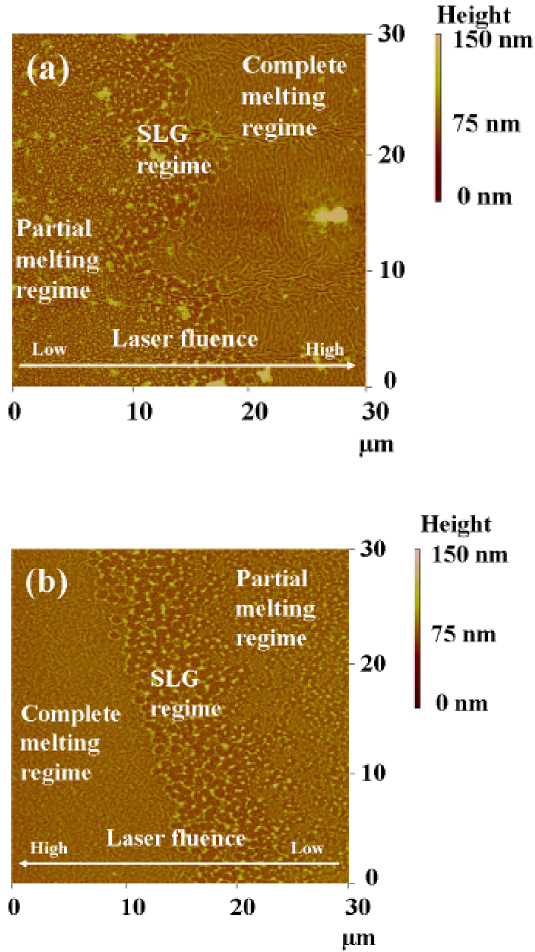

Fig. 3. Typical AFM micrographs of poly-Si films irradiated by the excimer laser energy density that causes the a-Si film complete melting for (a) frontside ELC and (b) backside ELC. Excimer laser energy density for frontside ELC and backside ELC is 210 mJ/cm^2 and 195 mJ/cm^2, respectively.

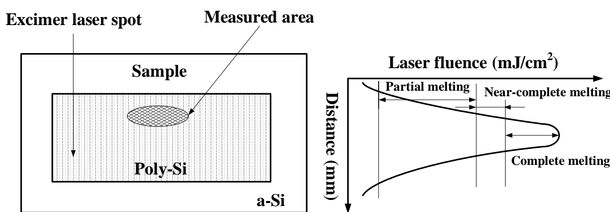

Fig. 4. Schematic illustration of the measured area.

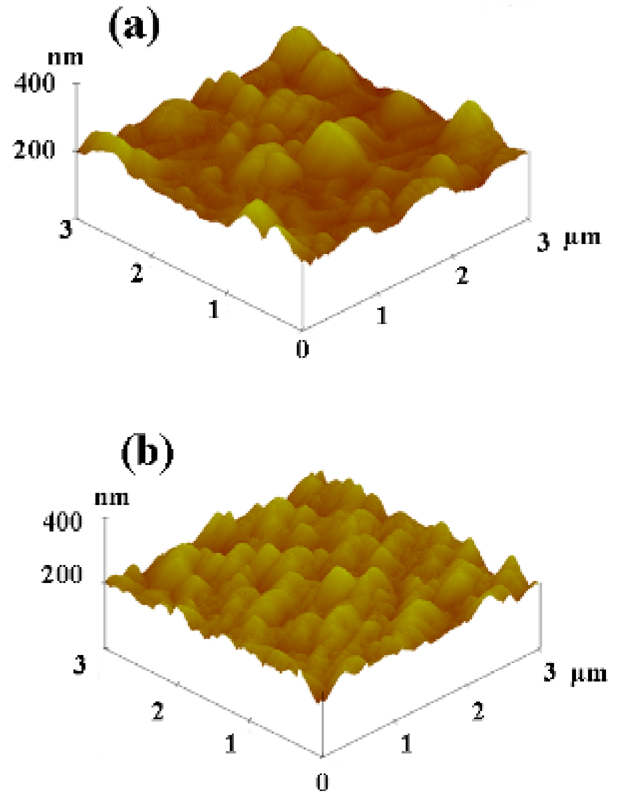

Fig. 5. Surface topography measured by AFM of poly-Si films in the SLG regime for (a) frontside ELC (RMS roughness= 21.192 nm) and (b) backside ELC (RMS roughness= 16.263 nm). Excimer laser energy density or frontside ELC and backside ELC is 190 mJ/cm^2 and 175 mJ/cm^2, respectively..

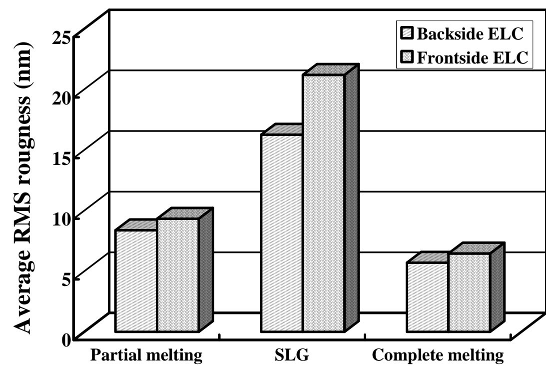

Fig. 6. Average surface roughness in the partial melting, SLG and complete melting regimes of Si thin films for frontside ELC and backside ELC. For frontside ELC, excimer laser energy density for parting melting, SLG, and complete melting regime is 130 mJ/cm^2, 190 mJ/cm^2, and 210 mJ/cm^2, respectively. For backside ELC, excimer laser energy density for the parting melting, SLG, and complete melting regime is 115 mJ/cm^2, 175 mJ/cm^2, and 195 mJ/cm^2, respectively. The area used for estimating RMS roughness is in the center of the spot size.

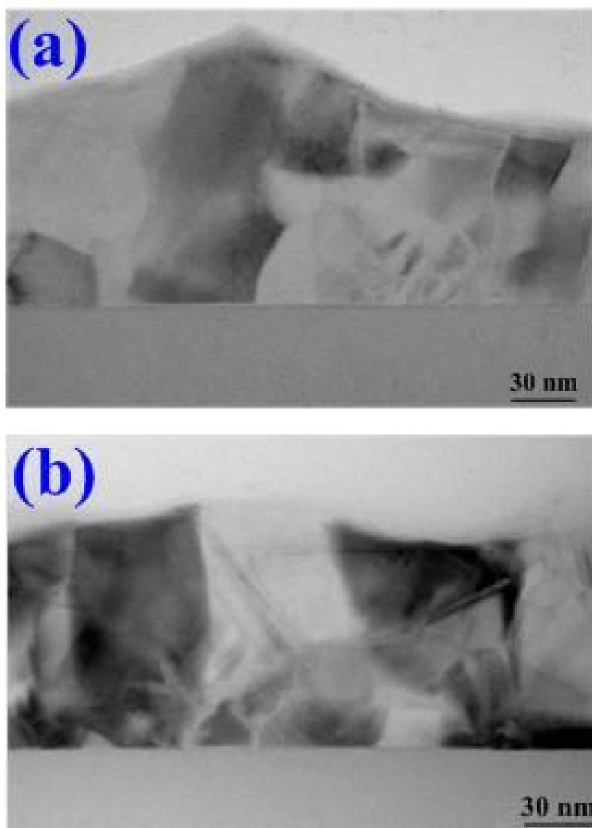

Fig. 7. Cross-sectional TEM images for (a) frontside ELC and (b) backside ELC. Excimer laser energy density for frontside ELC and backside ELC is 190 mJ/cm^2 and 175 mJ/cm^2, respectively.

Asai et al. [19] pointed out that the surface roughness of poly-Si films increases with the increase in grain size of poly-Si because surface roughness corresponds to grain size. Figure 8 shows the SEM micrographs of the complete melting of Si thin films for frontside and backside ELC. As can be seen, the maximum grain size of poly-Si films for frontside ELC and backside ELC are the same and the maximum grain size with a diameter of approximately 1 μm can be obtained by both frontside and backside ELC. Consequently, backside ELC is a better approach due to the lower surface roughness of poly-Si films. In addition, previous experimental results [20] revealed that backside ELC possesses higher laser efficiency than frontside ELC because this effect is mainly attributed to the anti-reflectivity characteristic of SiO_2 films for excimer laser beam [21]. According to the results described above, it is noteworthy that backside ELC seems to be a more promising approach for batch production of LTPS TFTs. High-quality poly-Si microstructure with lower surface roughness, lower intra-grain defect density, better crystallographic, and better uniformity is needed for the fabrication of high-quality LTPS TFTs. To enhance LTPS TFTs reliability and performance, some approaches to improving the surface roughness of poly-Si films have been proposed and described elsewhere [22-24].

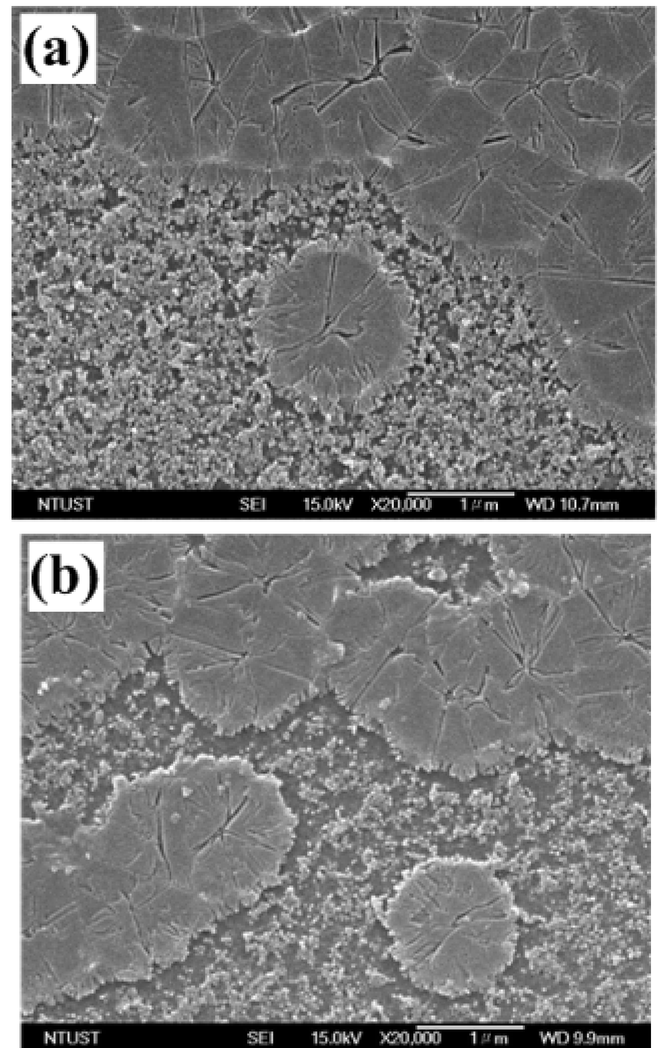

Fig. 8. SEM micrographs of complete melting of Si thin films for (a) frontside and (b) backside ELC. Excimer laser energy density for frontside ELC and backside ELC is 210 mJ/cm^2 and 195 mJ/cm^2, respectively.

4. Conclusions

Microstructural analysis of the resulting poly-Si films crystallized by both frontside ELC and backside ELC have been characterized by FE-SEM. The corresponding surface roughness of poly-Si films fabricated by both frontside ELC and backside ELC have been extensively investigated by AFM. The difference in surface roughness of poly-Si films between frontside ELC and backside ELC have been analyzed. The results showed that backside ELC leads to lower surface roughness of poly-Si films than frontside ELC in the partial melting, SLG and complete melting regimes. The RMS surface roughness of poly-Si films for frontside ELC and backside ELC in the SLG regime is 21.192 nm and 16.263 nm, respectively. It should be noted that backside ELC is strongly suggested for batch production of LTPS TFTs under the conditions including same maximum grain size of poly-Si films for both

frontside ELC and backside ELC, higher laser efficiency, and lower surface roughness of poly-Si films.

Acknowledgement

This work was financially supported by the National Science Council of Taiwan under Contract No. NSC 96-2221-E131-003.

References

[1] G. K. Giust, T. W. Sigmon, IEEE Trans. Elec. Dev. **47**, 207 (2000).
[2] Y. F. Chong, K. L. Pey, A. T. S. Wee, M. O. Thompson, C. H. Tung, A. See, Appl. Phys. Lett. **81**, 3786 (2002).
[3] A. T. Voutsas, Appl. Surf. Sci. **208**, 250 (2003).
[4] S. Friligkos,V. Papaioannou, J. Stoemenos, R. Carluccio,S. Cina, G. Fortunato, J.Cryst. Grow. **182**, 341 (1997).
[5] K. Nakazawa, J. Appl. Phys. **69**, 1703 (1991).
[6] J. S. Im, H. J. Kim, M. O. Thompson, Appl. Phys. Lett. **63**, 1969 (1993).
[7] J. S. Im, H. J. Kim, Appl. Phys. Lett. **64**, 2303 (1994).
[8] J. S. Im, R. S. Sposili, M. A. Crowder, Appl. Phys. Lett. **70**, 3434 (1997).
[9] D.K.Fork, G.B.Anderson, J.B. Boyce, R. I. Johnson, P. Mei., Appl. Phys. Lett. **68**, 2138 (1996).
[10] A. Shih, C. Y. Meng , S. C. Lee, M. Y. Chern, J. Appl. Phys. **88**, 3725 (2000).
[11] I. Asai, N. Kato, M. Fuse, T. Hamano, Jpn. J. Appl. Phys. **32**, 474 (1993).
[12] G. Fortunato, L. Mariucci, R. Carluccio, A. Pecora, V. Foglietti, Appl. Surf. Sci. **154**, 95 (2000).
[13] L. Mariucci, A. Pecora, R. Carluccio, G. Fortunato, Thin Solid Films **383**, 39 (2001).
[14] A. Pecora, R. Carluccio, L. Mariucci, G. Fortunato, D. Murra, S. Bollanti, P. Di Lazzaro, Thin Solid Films **427**, 319 (2003).
[15] B.Rezek, C.E.Nebel, M.Stutzmann, Jpn. J. Appl. Phys. **38**, L1083 (1999).
[16] C. C. Kuo, W. C. Yeh, J. F. Lee, J. Y. Jeng, Thin Solid Films **515**, 8094 (2007).
[17] C. C. Kuo, W. C. Yeh, C. B. Chen , J. Y. Jeng, Thin Solid Films **515**, 1651 (2006).
[18] L. Mariucci, R. Carluccio, A. Pecora, V. Foglietti, G. Fortunato, P. Legagneux, D. Pribat, D. Della Sala, J. Stoemenos, Thin Solid Films **337**, 137 (1999).
[19] I. Asai, N. Kato, M. Fuse, T. Hamano, Jpn. J. Appl. Phys. **32**, 474 (1993).
[20] C. C. Kuo, W. C. Yeh, C. P. Hsiao, J. Y. Jeng, J. Optoelectron. Adv. Mater. **9**, 2023 (2007).
[21] H.J. Kim, J. S. Im, Appl. Phys. Lett. **68**, 1513 (1996).
[22] E. Fogarassy, J. Venturini, J. Korean Phys. Soci. **48**, 40 (2006).
[23] A. Pecora,L. Mariucci, S. Poperno, G. Fortunato, Thin Solid Films **427**, 314 (2003).
[24] C. Y. Chang, H. Y. Lin, T. F. Lei, IEEE. Elec. Dev. Lett. **17**, 100 (1996).

Corresponding author: jacksonk@mail.mcut.edu.tw